Journal of Mechanical Engineering Research and Developments
ISSN: 1024-1752
CODEN: JERDFO
Vol. 43, No. 2, pp. 349-360
Published Year 2020

Static aeroelastic approach based on Vortex lattice Method and Euler-Bernoulli beam theory for structural analysis of fixed wing sUAS.

Esteban A. Valencia*, Alexander F. Ramos, Víctor H. Alulema & Darío A. Rodríguez

Escuela Politécnica Nacional, Departamento de IngenieríaMecánica, Quito, Ecuador, 17-01-259

*Email: esteban.valencia@epn.edu.ec

ABSTRACT: Unmanned Aerial Vehicles performing in the Andean Region (3000-5000 m.a.s.l) impose different operating requirements for the structural design due to the harsh atmospheric conditions. At preliminary design stage where various configurations need to be tested, it is needed a versatile and low-cost computational method to assess the structural behaviour of Small Unmanned Aerial System (sUAS) in the aforesaid demanding operating conditions. In this regard, this work develops a static aeroelasticity method adapted for the case of sUAS, which is accurate enough to capture main trends in material performance and geometrical features. This method is based on the well-known Vortex Lattice Method for the aerodynamic force assessment and uses the Euler-Bernoulli beam theory to evaluate the static aeroelasticity of the sUAS concepts. Results were contrasted with open-access information and comparison showed that the proposed method reproduces static aeroelasticity phenomena with good accuracy. Afterwards, a study case using a sUAS concept developed in previous works was analyzed operating in the pilot zone at the Andean Region in order to evaluate wing deflections.

KEYWORDS: sUAS; static aeroelasticity; Andean Region

INTRODUCTION

The high altitude of the Andean Region (3000 - 5000 m.a.s.l) has a particular behavior in temperature and wind patterns, presenting warm, moist and rainy conditions, climatological features which hinder the operation of small unmanned aerial systems (sUAS) with severing troubles regarding to performance [1, 2]. Therefore, it is required to improve aircraft design methods, which should be versatile and allow an easy coupling to analyze several phenomena at once in order to enable selection and usage of good enough architectures of sUAS [3]. This approach could be developed by a multidisciplinary analysis focused on the interrelation of all main sciences, some of which are aerodynamics, structures, weight and propulsion [4, 5]. This work mainly deals with the structural assessment at static conditions and is based on previous works that have studied the remaining systems [6-9]. Accordingly to Dowell et al [10], aeroelasticity is concerned with those physical phenomena which involve an interaction between inertial, elastic and aerodynamic forces. The stability of a structure such as an aerial planform is critically related to lift loading which increases with cruise speed [11, 12]. Hence is imperative to set up operating conditions in order to find the effect of elastic deformation occurred by these aerodynamic forces over the wing and determine the critical speed at which the structure becomes unstable and may lead to its destruction [13]. Nevertheless, aeroelasticity could be formulated such as static and dynamic assessments. Static aeroelasticity is a coupled problem where aerodynamic forces and an elastic body is modeled as a solid mechanic phenomena. Varello et al. [14]investigated a refined beam model for linear static aeroelastic analysis through a beam-like structures, the linear steady aerodynamic loads are described by the Vortex Lattice Method (VLM) developed by Lamar and Margason [15] and the coupling of structural – aerodynamic fields was performed by a Complex Beam Theory, either way this method requires a great computational cost due to high accuracy which can offers. Lee et al. [11] realized a similar analysis considering dynamic aeroelasticity using a panel method to solve the aerodynamic forces and a commercial software for the structural design. However, the black box structure of the commercial software constrains up to certain limit its versatility for certain analysis. Hall [16] studied the aeroelastic response of an actively controlled flexible wing through Euler- Bernoulli beam approach with modal response, and a nonlinear unsteady VLM for the aerodynamic response, both coupled by a boundary approach. In fact Hall method represents a successful solution when an analysis of static and dynamic aeroelasticity such as flutter oscillations of the wing or gusts analyses are required. Based on the satisfactory results of the aforesaid method, the present work uses a similar path where a linear steady VLM is employed to determine aerodynamic loading at subsonic speeds and the Euler-Bernoulli beam theory are

implemented for the static analysis without regard to modal analyses. To reduce computational cost the present model adapts the Hall and Varello et al. approach, by shifting the way of coupling the structural and aerodynamic modules, and the development of a simplest methods referred to structural and aerodynamic modules. Varello et al. and Hall uses an extrapolation of the structural grid (one dimensional) onto the aerodynamic grid (two dimensional) to project the aerodynamic loads, whereas the current model modifies the punctual aerodynamic loads into a distributed load reducing the two-dimensional problem to one dimensional. This distributed load then is transformed into a system of equivalent forces (loads and nodal moments), which are inserted into the one-dimensional structural grid. Furthermore, this work adapts the aforementioned methods for the case of sUAS, since most of the works developed in this subject focus mainly on civil aviation, and hence the materials and correlations differ from the required for other aviation sectors, also the main advantage of this method lies in that can be implemented in a frame of optimization, where the computational costs reduction is desired.

METHODOLOGY

This work presents a highly versatile and accurate enough method to estimate, at preliminary design stage, structural deflections on aircraft wing occurred by static aeroelasticity phenomena. The proposed method couples, in a single tool, the aerodynamic and structural assessment for the aeroelastic evaluation of aircraft wing, which has been adapted for the case of sUAS.For the aerodynamic analysis, the Vortex Lattice Method is employed to determine the aerodynamic characteristics of a planform at subsonic speeds. Then, Euler-Bernoulli beam theory coupled to VLM is utilized to calculate the structural deflections of the wing, which is modelled as a cantilever beam under bending loads without torsion approach.

In the next subsections further description is presented about the aerodynamic and structural modules.

Aerodynamic Model

The Vortex Lattice Method has been extensively used for the aerodynamic evaluation of lifting surfaces due to represent the simplest method of surface panel methods to predict subsonic characteristics considering an incompressible potential flow (inviscid, irrotational and isentropic) [15, 17]. The lifting surface solution is represented by a twisted and cambered wing as a planar surface with linearized boundary conditions, considering a grid of vortex ring elements. The singularity element is based on the vortex line solution of the incompressible flow theory, and the boundary condition satisfied by the solution is the zero normal flow across the wing surface [18].

According to the methodology flowchart of the Figure 1, to solve VLM is necessary to discretize the wing geometry in N and M panels along the spanwise and chordwise directions respectively, *y* and *x* direction as shown in Figure 2.

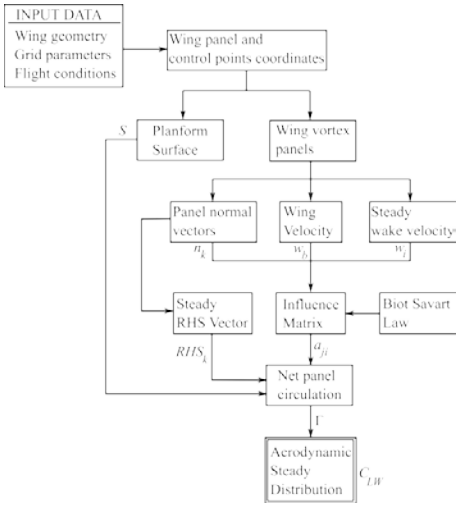

Figure 1. Aerodynamic model methodology.

Later, should be calculated the wing panel and control points coordinates in order to evaluate the wing vortex panels. The normal vectors are calculated through the Equation(1)where two vectors, A_k and B_k, are defined

over the opposite corner points of the discretized panel of the wing. The zero normal flow boundary condition across the wing surface is attached to calculate the wing velocity induced by a rectilinear vortex ring, each one composed of a straight vortex segment [18].

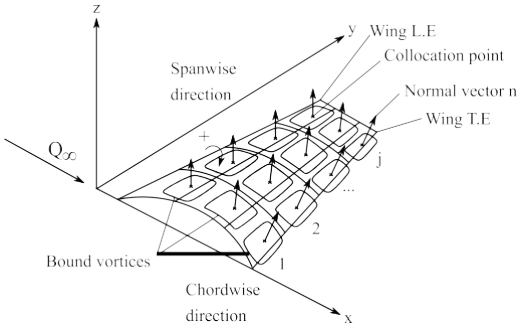

Figure 2. Vortex ring model for a thin lifting Surface [18].

$$n_k = \frac{A_k \text{x } B_k}{|A_k \text{x } B_k|} \tag{1}$$

The influence coefficients are calculated computing the dot product of the induced velocity of a particular vortex ring and its normal vector. The induced velocity and collocation points are obtained owing vortex strength as show in Equation (2). To form the right-hand side vector (RHS), the dot product of the normal velocity component of the free stream flow and the normal vector are calculated over Equation (3). Eventually, Equation (4) derives a system of linear equations, where *m* is the total number of vortex rings. Solution yields the amount of the vortex strength for each panel Γ. Finally, to estimate the steady lifting distribution, the Kutta-Joukowski theorem is applied into the Equation (5) to estimate the aerodynamic distribution ΔL [19].

$$a_{ij} = (u, v, w)_{ij} \cdot n_i \tag{2}$$

$$RHS = -Q_\infty \cdot n_i \tag{3}$$

$$\begin{pmatrix} a_{11} & a_{12} & \cdots & a_{1m} \\ \vdots & \vdots & \ddots & \vdots \\ a_{m1} & a_{11} & \cdots & a_{mm} \end{pmatrix} \begin{pmatrix} \Gamma_1 \\ \vdots \\ \Gamma_m \end{pmatrix} = \begin{pmatrix} RHS_1 \\ \vdots \\ RHS_m \end{pmatrix} \tag{4}$$

$$\Delta\mathcal{L} = \rho Q_\infty \Delta\Gamma\Delta\text{y} \tag{5}$$

Structural assessments of an aerial platform (wing) requires aerodynamic loads, geometry and mechanical properties to evaluate static or dynamic aeroelasticity. Since most of structural high-fidelity methods require large computational costs, it is desirable to reduce complexity by assessing aeroelasticity problems with numerical methods in one dimensional framework. Euler - Bernoulli beam theory allows to model the behavior of a lineal - elastic girder perpendicular to its axis, this principle can be observed in Figure 4, where is represented a cantilever beam with a point load *P* . This bending deformation is measured as a transverse displacement *v*(x) and a rotation $\emptyset(x)$ [20, 21]. Regarding to the Finite Element Methods (FEM), is accurate to relate nodal forces to nodal displacements carried out by bending approach such as Euler - Bernoulli model. Equation (6) represents the system of equations, described by the transverse forces, bending moments, transverse displacements, rotations and stiffness matrix to obtain a simple analysis of FEM, whereas axial effects have been neglected [21-23]. Flowchart of Figure 3 presents how can be carried out structural assessment.

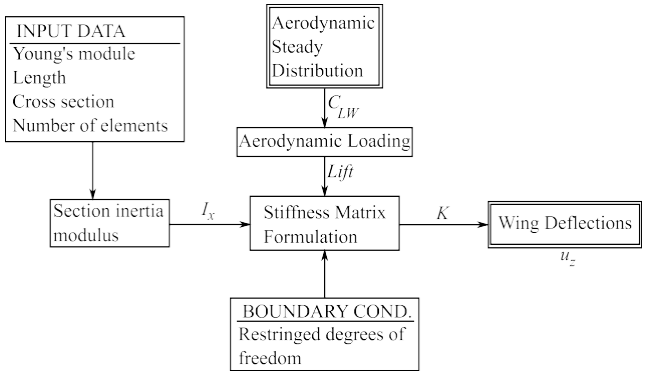

Figure 3. Structural model methodology.

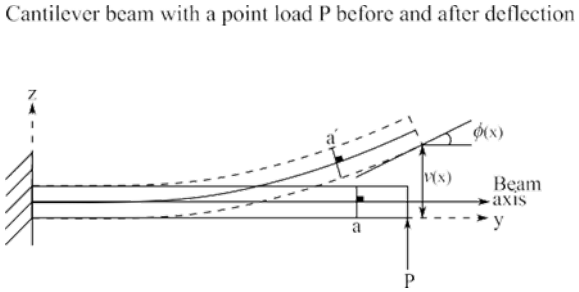

Figure 4. Euler - Bernoulli beam theory representation.

Aeroelasticity Approach

Static aeroelasticity is interrelated through two mathematical models, aerodynamic and structural, which need to be coupled. In order to identify this relation, an assumption is chosen to adapt and study structural phenomena. Lift distribution is identified with an elliptical - parabolic behavior due to the approach that maintains VLM and wing geometry, which results in minimum drag and a constant downwash to avoid stall condition [18, 24]. In brief, lift is approximated by a system of statically equivalent forces shaped by loads and nodal moments. Logan [21] developed an analysis of beams with FEM solution, where a specific distributed load can be transformed to a single equivalent element join forces $f_{n,y}$ and m_n. Figure 5 illustrates a distributed loading q over a cantilever beam of length l related to bending effects and summarizes the equivalent joint forces which can be used to transform a distributed loading to a single element with 2 nodal forces and moments.

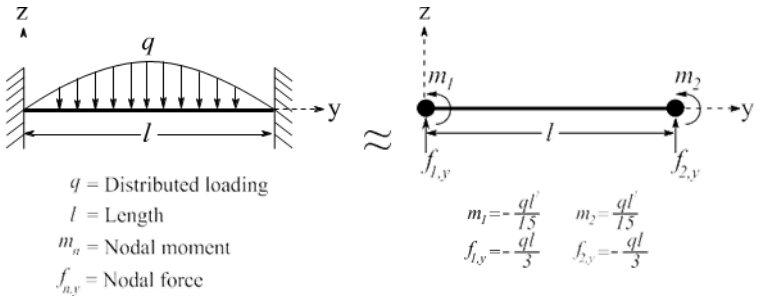

Figure 5. Scheme of distributed loading to single element join forces.

Analogous, it has been assumed the wing as a cantilever beam made of an uniform solid material, with a constant cross section corresponding to an airfoil [14]. Therefore, according to Drela et al. [25], the moment of inertia of an airfoil section can be computed through a smooth geometry as shown in Figure 6. The airfoil shape given by the upper and lower surfaces $Z(x)$ and $Z(x)$ are related to the inertia occurred about the bending axis x. Hence, the area A and the total bending inertia I are the contributions of all the infinitesimal sections dx associated to the neutral surface position z. To define the relations which describes bending inertia for common airfoils, is necessary to approximate A and I through the geometry airfoil properties such as maximum thickness t, and maximum camber h. A and I are proportional to the following approximations, where the coefficients K_A and

K_I can be evaluated for the most common airfoil shapes (Equation (7) and (8)), which are functions of the airfoil geometry and are related that the bending deflection will occurs in the z direction.

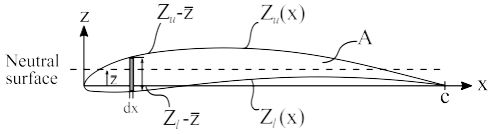

Figure 6. Quantities for determining and estimating the bending inertia of an airfoil section [25].

RESULTS AND DISCUSSION

This section shows firstly a comparison of the models described against literature available in the open domain. Then it describes the case of study where the current model has been tested for the static structural assessment of a sUAS operating in the Andean region.

Aerodynamic model comparison

Results obtained for aerodynamic model were contrasted with the work developed by Katz [26], where an analysis of the effect of wing sweep on the spanwise loading of untapered planar wings is discussed. A planar wing with $AR = 4$ is considered for different sweep angles Λ. Figure 7 shows that the aft-swept wings have an increase in lift toward tip chord, while forward-swepts wings present a raising lift loading near the root chord due to downwash induced by the right wing vortex [18]. In summary, the rate between the local lift coefficient C_l and the total lift coefficient C_{LW} considered for swept and unswept wings present an error which oscillate between 2.53 and 1.08%, modelled with the present model (VLM) and the work of Katz [26]. The discrepancies between both models are small and are related to the accuracy of the model which was developed in open source Python programming language.

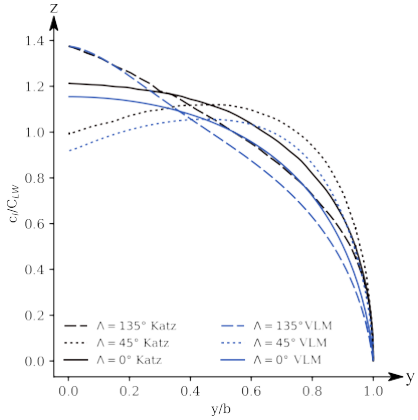

Figure 7. Comparison of spanwise loading of swept and unswept rectangular wings.

Structural model comparison

For structural model, is considered a beam with a rectangular cross-section with 3x60[mm], length L = 600[mm], Young's modulus E = 69[GPa] and a concentrated bending load P = 1 [N]. The phenomena occurred is described in terms of dimensionless maximum vertical displacement (u_{max}) and compared with the work developed by Varelllo et al. [14], the present FEM Euler-Bernoulli model and the solution given by the classical beam theory, which is taken as reference u_{max} =7.73 [mm]. In brief, for the values of structural deflections, the maximum displacement occurs at the tip of the beam. Furthermore, the Euler-Bernoulli model has a low reproduction error corresponding to 0.38 and 0.12 %, compared to the classical beam theory and the work of Varello et al. Results do not present significant differences due to simplicity of the FEM model and its formulation is originated from the classical beam theory approach.

Aeroelastic model comparison

The aeroelastic assessment has the aim to validate the aeroelastic model by comparison with the work developed

by Varello et al. [27]. Here is considered a wing with a constant cross-section equivalent to an airfoil, the baseline configuration is contemplated with a sweep angle $\Lambda = 0°$, taper ratio $\lambda = 1$, the same root and tip chord $C_r = C_t = 1$, spanwise $b = 10\ [m^2]$, surface area $S = 10\ [m^2]$, aspect ratio $AR = 10$, Young's modulus $E = 69\ [GPa]$ and an airfoil NACA 2415. Figure 8 shows the effect of the free stream velocity on the maximum transverse displacement at the 10 □ 40 $[m\ /\ s]$ tip cross-section. The analysis was realized in a range of velocity corresponding to and an altitude of $0\ m.a.s.l$. The rise in the deflections are induced by the change of spanwise loading, when speed increases the variation among the present work and Varello et al. increases. This higher difference is related to the considerations assumed in VLM, nevertheless an acceptable margin with an error of 11.86 % is maintained. Regarding to the maximum transversal displacements, at high velocities exists a maximum deflection of $140\ [mm]$ at the tip corresponding to a velocity of $40\ [m\ /\ s]$.

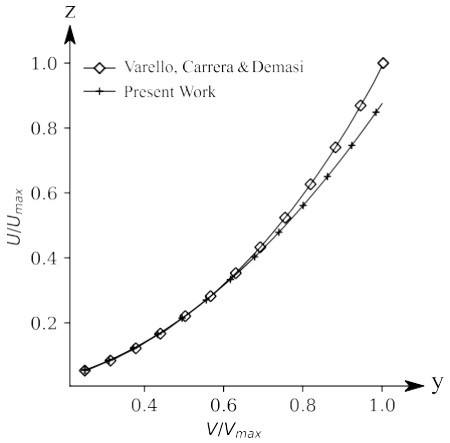

Figure 8. Effect of free stream velocity above maximum transversal displacement.

Convergence analysis

For the previous validation assessments, a convergence analysis needs to be realized, and set up the number of elements or panels required to achieve the present study with good accuracy. According to the typical behavior of FEM, the maximum tip displacement increases and becomes more truthfulness such as the number of elements N increases, but if is selected a higher number N, computational cost raises significantly. Corresponding to the aerodynamic and aeroelasticity models a related response occurs.

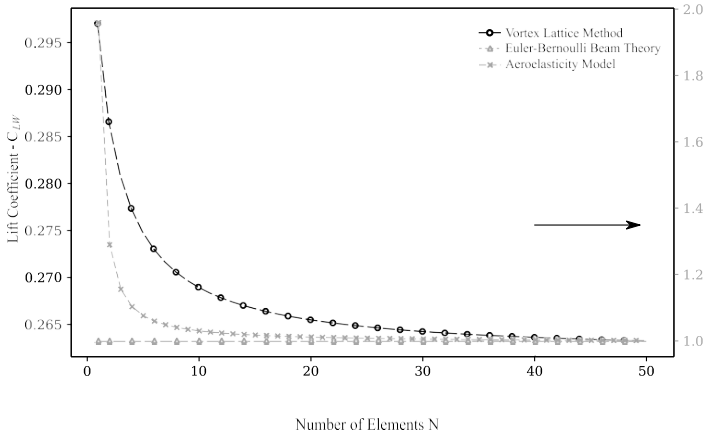

(a) Convergence analysis of the number of elements N referred, to the structural, aerodynamic and aeroelasticity models.

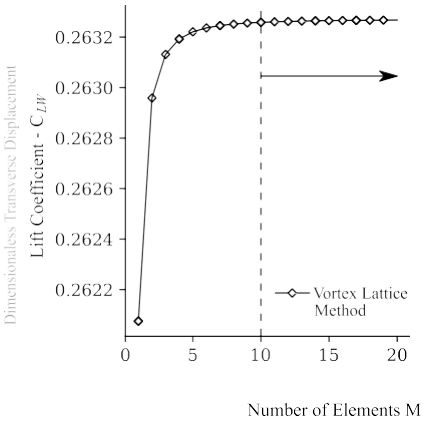

(b) Convergence analysis of the number of elements M referred to the aerodynamic model.

Figure 9. Convergence analysis.

Figure 9(a) describes behavior of solution for the aforementioned methods meanwhile the number of elements boosts. Anyway, is proved graphically that the convergence on N is reached at 40 to 50 elements. Moreover, is required to set the number of panels M among the chord direction for the aerodynamic model, Figure 9(b) shows that solution is achieved at 5 panels, when the variation in lift coefficient is not meaningful.

Study case

The study case for this work is the implementation of a sUAS for precision agriculture and monitoring tasks suitable for the Andean region [7-9]. The baseline airframe configuration was selected from a previous work were the basic geometrical features were determined [7]. Table 1 presents the geometrical parameters considered. The analysis for the case of study is categorized in operating conditions, material properties and geometrical configuration. For each assessment the same baseline configuration is used

Table 1. Baseline sUAS parameters.

Parameter	Value
b [m]	3.32
S [m^2]	2.00
AR	5.5
C_r [m]	0.72
C_t [m]	0.72
Λ [deg]	2.5
Maximum speed [m / s]	48 (0.145 Ma)

In this section is presented the effect of the AoA above the aerodynamic loading and displacements along the wing. Generally an elliptical trend distinctive of a lifting surface can be observed, hence the lift loading is currently presents the same trend such as reported in the distribution of the lift coefficient as shown inFigure 10. For small attack angles it is evident a lower lift coefficient distribution, which is connected to the lower lift in comparison to higher AoA cases. For this study, the AoA is based on the work of Valencia et al. [7] where an angle of attack of 2° is calculated for cruise condition. Consequently, in an interval of 1° to 3° exist a raise onto the lift coefficient and lift loading which presents suitable structure deflections in contrast whit higher attack angles. In the next assessments, an AoA equivalent to 3° is arranged.

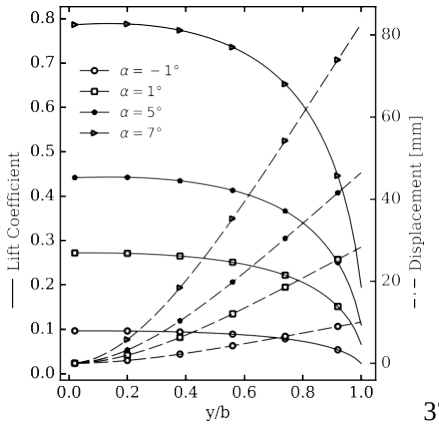

37

Figure 10. Effect of lift coefficient and structural displacements along spanwise with a variable angle.

In Table 2 the maximum transversal displacement for each angle of attack is shown. To assess how acceptable the maximum displacements are within the wing geometry, the VLM model was run based on the structural affected geometry and based on the displacements obtained (AoA of 2° with a deflection of 45.56 mm) it was observed non-significant variations on the aerodynamic assessment model.

Table 2. Effect of attack angle referred to static aeroelasticity approach.

α **[deg]**	C_{LW}	**L [N/m]**	u_{max} **[mm]**
-1	0.09	236.90	10.05
1	0.27	667.45	28.31

5	0.44	1086.58	46.48
7	0.78	1935	82.77

Figure 11 shows the results for lifting distribution and deflections over the wing with respect to altitude. The loading distribution shows a variation, at high altitudes (5000 m.a.s.l) there is a reduction due to the lower air density. The same criteria is applied in the structural displacement assessment.

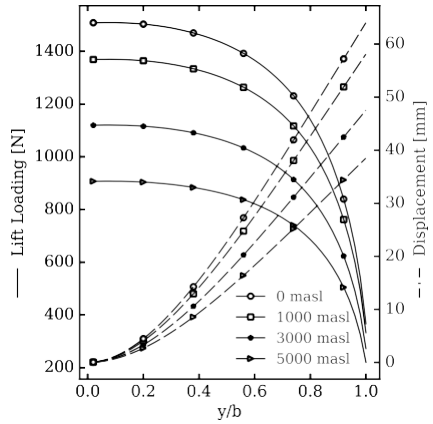

Figure 11. Effect of lift loading and structural displacements along spanwise with a variable altitude.

Finally, Table 3shows the lifting distribution above the wing for a range of altitudes, and its corresponding transversal displacement. It is notorious that for the Andean Region wing displacements do not represent a significant problem but is visible that velocity has an influence above the wing structure. The highest displacement occurs when the sUAS flies at low altitudes and high velocities. However, in this critical scenario the maximum displacement is still within the margin of do not affecting largely the aerodynamic loads.Flight velocity is an important variable which will need to be considered in dynamic analysis. For the next sections an operating altitude of 3200 m.a.s.l.

Table 3. Effect of altitude referred to static aeroelasticity approach.

Altitude [m.a.s.l]	**L [N/m]**	**u_{max} [mm]**
0	1509.38	64.04
1000	1369.73	58.11
3000	1120.34	47.53
5000	907.39	38.49

Material properties

To assess the static aeroelasticity phenomena, a set of polymeric materials are evaluated through Young's Modulus showed inTable 4[28]. Furthermore, the investigation is performed considering elastic and linear response with an isotropic material behavior. Most of sUAS material are not isotropic, however this first assumption was taken in order to reduce the complexity of the present model, in future studies is envisioned to incorporate this feature into the structural module. Figure 12 exhibits the displacements occurred over the structure. As expected, as Young's module increases, the deflections decrease but the material weight increases because of material density and stiffness. From this analysis polystyrene was selected for the next sections, due to its benefit in weight, strength, maneuverability and costs in comparison with the other materials.

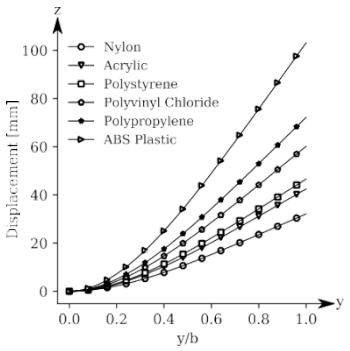

Figure 12. Effect of transversal displacement for different materials.

Table 4. Material properties and effect of maximum transversal displacement [28].

Material	**Young's Modulus E [GPa]**	**u_{max} [mm]**
Nylon	4.5	32.07
Acrylic	3.4	42.45
Polystyrene	3.1	46.56
Polyvinyl Chloride	2.4	60.14
Polypropylene	2	72.17
ABS Plastic	1.4	103.10

Geometric parameters

According to the work developed by Valencia et al. [7], the baseline model was included in an analysis to evaluate the performance of several aerodynamic profiles. The NACA 2415, NACA 4412 and SD 7032 was analyzed by using a semi-empirical chart presented by Sadraey [29]and modified to include low-Reynolds numbers.

Table 5. Airfoils parameters and effect of maximum transversal displacement.

Airfoil	**Thickness t[%]**	**Camber h[%]**	**u_{max} [mm]**
NACA 4412	12	4	27.05
SD 7032	10	3.4	45.56
NACA 2415	15	2	15.12

Finally, the SD 7032 due to the excellent aerodynamic characteristics as highest lift coefficient, maximum lift slope and minimum drag coefficient at cruise condition was selected to model the wing. Table 5and Figure 13shown the main airfoil parameters considered and the distribution of structural deflections along the aircraft. It is observed that the SD 7032 presents the longer deflections in contrast to NACA 2415 and NACA 4412, nevertheless owing to the best aerodynamic performance presented by SD 7032 and the small variations in regard of the aerodynamic loading distribution this airfoil was selected for the next sections.

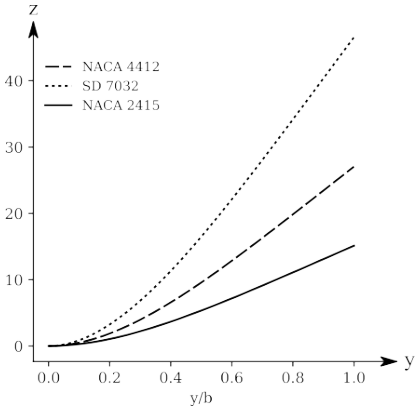

Figure 13. Effect of transversal displacement for different airfoils.

The last parameter which was analyzed is the sweep angle Λ, and describes the behavior of the aerodynamic distribution and structural displacements for a range of angles between 0 – 45°, additionally, the analysis is considered to assess the correlation between displacements and Λ, however the baseline geometry specifications of the work by Valencia et al. [7]is maintained in the whole case study. Figure 14 illustrates elliptical distributions at lower sweep angles. As observed from this graph a higher sweep angle would represents benefits to reduce the maximum structural displacements, which is related to the lower lift loading. This presumption is correlated by the results showed in Table 6.

Table 6. Effect of sweep angle referred to static aeroelasticity approach.

Λ [deg]	**C_{LW}**	**L [N/m]**	**u_{max} [mm]**
0	0.45	1109.26	46.59
20	0.41	1018.17	44.76
30	0.38	954.51	42.36
45	0.33	816.89	34.61

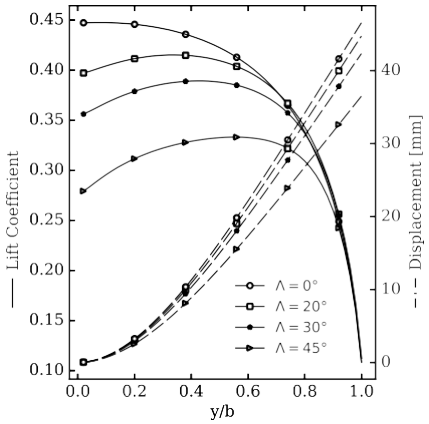

Figure 14. Effect of lift coefficient and displacements along spanwise with a variable sweep angle.

To summarize from the previous cases assessed can be observed that the model predicts with good accuracy the trends expected for the structural behavior of the wing, however the variations in its deflection are far from causing a structural damage at static conditions. Figure 15 only illustrates the wing of the sUAV affected by structural deflections analyzed in the present work.

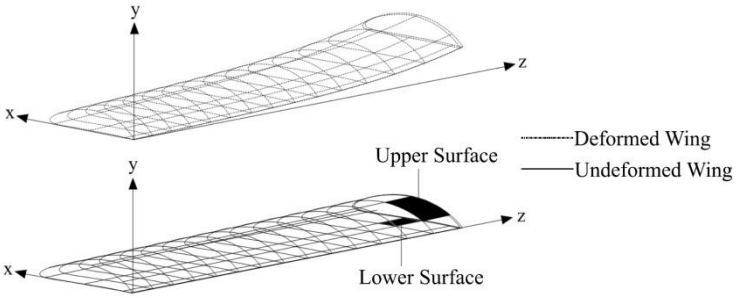

Figure 15. Aeroelastic deflection above the wing of the sUAS analyzed.

CONCLUSIONS

Static aeroelasticity phenomena in a sUAV for SSM in the Andean region was studied. The performance of its phenomena was attended in order to define a suitable method using an adapted and novel methodology through the well-known VLM and Euler-Bernoulli beam theory. Results were contrasted with open-domain information and differences are less than 13 %. Comparison of models showed that the proposed method reproduced the static aeroelasticity problem with good accuracy and low computational demand. Furthermore, a previous developed UAV was assessed structural statically in the Andean region and from the studies is evident

that there is not a significant variation of the wing loading due to the static deformations of well-known implemented materials in the sUAS sector. Nevertheless, it is required to further refine the model for anisotropic materials and dynamic analysis (flutter oscillations and gusts).

ACKNOWLEDGEMENTS

The authors gratefully acknowledge the financial support provided by Escuela Politécnica Nacional for the development of the project PIJ 15-11, PIS 16-20, PIMI 15-03, PIMI 18-01, PIE-CEPRA-XII-2018-12 and the support of Group FARO \& FFLA organization.

REFERENCES

[1] R. D. Garreaud, "The Andes climate and weather", *Adv. Geosci.*, 2009.

[2] R. Garreaud, M. Vuille, y A. C. Clement, "The climate of the Altiplano: Observed current conditions and mechanisms of past changes", en *Palaeogeography, Palaeoclimatology, Palaeoecology*, 2003.

[3] K. P. Valavanis y G. J. Vachtsevanos, *Handbook of unmanned aerial vehicles*. 2015.

[4] J. P. Fielding, *Introduction to Aircraft Design*. 2012.

[5] C. Haberland, W. Fenske, y J. Thorbeck, "A computer-augmented procedure for commercial aircraft configuration development and optimization", *J. Aircr.*, 2008.

[6] E. Valencia, V. Alulema, y D. Rodríguez, "Wetland Monitoring Using Unmanned Aerial Vehicles with Electrical Distributed Propulsion Systems", en *Propulsion Systems [Working Title]*, 2019.

[7] E. A. Valencia, V. Hidalgo, y D. Rodriguez, "Parametric modelling for aerodynamic assessment of a fixed wing UAV implemented for Site Specific Management", en *2018 AIAA Information Systems-AIAA Infotech @ Aerospace*, 2018.

[8] E. Valencia, V. Hidalgo, y O. Calle, "Weight and Performance Methodology of an UAV at Cruise Condition for Precision Agriculture", *AIAA Pap.*, no. August, pp. 1–15, 2017.

[9] E. Valencia, V. Hidalgo, y J. Cisneros, "Design point analysis of a distributed propulsion system with boundary layer ingestion implemented in UAV's for agriculture in the Andean region", en *52nd AIAA/SAE/ASEE Joint Propulsion Conference*, 2016.

[10] E. H. Dowell, R. H. Scanlan, F. Sisto, H. C. Curtiss, y H. Saunders, "A Modern Course in Aeroelasticity", *J. Mech. Des.*, 2010.

[11] I. Lee, H. Miura, y M. K. Chargin, "Static Aeroelastic Analysis for Generic Configuration Aircraft", *NASA Tech. Memo.*, p. 53, 1987.

[12] R. Bisplinghoff, Raymond; Ashley, Holt; Halfman, *Aeroelasticity*. New York: Dover Publications, 1983.

[13] Y. Fung, "An Introduction to the Theory of Aeroelasticity". Dover Publications, New York, p. 498, 1983.

[14] A. Varello, L. Demasi, E. Carrera, y G. Giunta, "An improved beam formulation for aeroelastic applications", *Collect. Tech. Pap. - AIAA/ASME/ASCE/AHS/ASC Struct. Struct. Dyn. Mater. Conf.*, no. April, p. 3032, 2010.

[15] R. J. Margason y J. E. Lamar, "Vortex Lattice Fortran Program for Estimating Subsonic Aerodynamic Characteristics of Complex Planforms", 1971.

[16] B. D. Hall, "Numerical Simulations of the Aeroelastic Response of an Actively Controlled Flexible Wing", Virginia Tech, 1999.

[17] R. J. Margason, S. O. Kjelgaard, W. L. Sellers, C. E. K. Morris, K. B. Walkley, y E. W. Shields, "Subsonic Panel Methods - A Comparison of Several Production Codes", *23rd Aerosp. Sci. Meet. AIAA*, 1985.

[18] J. Katz y A. Plotkin, "Low Speed Aerodynamics", *McGrawhill Inc*, no. February 2013, p. 351, 1991.

[19] J. R. Wright y J. E. Cooper, *Introduction to Aircraft Aeroelasticity and Loads: Second Edition*. 2015.

[20] J. Almeida, “Structural Dynamics for Aeroelastic Analysis”, Técnico de Lisboa, 2015.

[21] D. L. Logan, “A First Course in the Finite Element Method”. CENGAGE Learing, p. 937, 2012.

[22] J. N. Reddy, “An Introduction to the Finite Element Method”. Mc Graw Hill, p. 684, 1993.

[23] K. J. Bathe, *Finite Element Procedures*. New Jersey: Prentice Hall, 1995.

[24] J. J. Bertin y R. M. Cummings, *Aerodynamics for Engineers (Fourth Edition)*. Pearson, 2001.

[25] M. Drela *et al.*, “Area and Bending Inertia of Airfoil Sections”, 2005. Available in: https://ocw.mit.edu/courses/aeronautics-and314%0Aastronautics/16-01-unified-engineering-i-ii-iii-iv-fall-2005-spring-2006/systems-labs-06/spl10b.pdf. [Online: accessed 05-November-2018].

[26] J. Katz, “Calculation of the Aerodynamic Forces on Automotive Lifting Surfaces”, J. Fluids Eng., vol. 107, no. 4, p. 438, 1985.

[27] A. Varello, E. Carrera, y L. Demasi, “Vortex Lattice Method Coupled with Advanced One-Dimensional Structural Models”, *ASDJournal*, vol. 2, no. 2, pp. 53–78, 2011.

[28] M. A. Meyers y K. K. Chala, *Mechanical behavior of materials*. Cambridge University Press, 2008.

[29] M. Sadraey, *Aircraft Design*. John Wiley & Sons, Ltd, 2013.